

# *Molecular dynamics simulation of self-assembly in anionic and zwitterionic surfactant systems*

Lingchi Xu

*College of Materials Science and Engineering, South China University of Technology, Guangzhou, Guangdong, 510640, China*

**Keywords:** Self-assembly, simulation, surfactant

**Abstract:** To explore the rheological behavior of anionic/zwitterionic surfactant mixtures, we performed molecular dynamical simulations at different molar ratios ( $X_{\text{TPS}} = [\text{TPS}]/([\text{TPS}]+[\text{SDS}])$ ) and  $\text{Ca}^{2+}$  concentration of sodium-dodecyl-sulfate (SDS) and tetradecyl-dimethyl-ammonium-propane-sulfonate (TPS) aqueous mixtures, which were investigated previously in experiment [1]. The simulation results indicated that with the increase of  $X_{\text{TPS}}$ , the micelle aggregation evolving path is interdigitate-wormlike-sphere. Furthermore, with increasing  $\text{Ca}^{2+}$  concentration, the micelle aggregation evolving path is also interdigitate-wormlike-sphere. We can conclude that there exist an appropriate molar ratio and salt concentration to form wormlike micelle in the anionic/zwitterionic systems.

## 1. Introduction

Surfactant can spontaneously self-assemble into a wide variety of micellar structures such as spherical, wormlike, vesicle, lamellae or bilayer phases [2-5] in solutions due to the coexistence of both hydrophilic head groups and hydrophobic tail in the molecule. The structural phase of micelle depends sensitively on the molecular structure, concentration, salt, and temperature/PH. Because of the fascinating structural characters and rheological properties, micelle has a wide range of applications such as viscosity enhancers, cosmetics, drug delivery, personal care products [6-8]etc. To investigate the microscopic nature of the aggregates and understand the formation of aggregates in solutions, many modern experimental techniques, including Raman scattering, nuclear magnetic resonance, light scattering and small angle neutron scattering have been used[9-14].

In recent years, due to the substantial increase in computational power, computer simulations such as Monte Carlo (MC)[15,16] and Molecular dynamics (MD)[17-20] have proved to be a powerful tool in analyzing microscopic details and dynamics properties of aggregates at atomic level. In the past decades, many molecular dynamics simulation research have been utilized to study self-assembly in surfactant solutions. H. T. Davis[21], Wang ZW[22], and Sangwai AV[23,24] have studied the properties of cationic surfactant  $\text{CTA}^+$  in the presence of NaCl and NaSal salt, the Sal- ion is known from simulations to facilitate the spherical to wormlike micelle transition. Sammalkorpi et al. [25,26] have studied the influence of temperature and inorganic salt to the anionic surfactant SDS solutions. They found SDS surfactants form crystalline aggregate at low temperatures and micelles at elevated temperatures, the adding inorganic ions especially  $\text{Ca}^{2+}$  can induce more compact and densely packed micelles. Velinova Maria[27] use coarse-grained molecular dynamics simulation to describe micellar

assemblies of nonionic surfactant pentaethylene glycol monododecyl ether (C12E5) at different concentrations. With the increase of surfactant concentration, the spherical to rod-like aggregates transition is observed. Zana et al[28] have proved that cationic gemini surfactant alkanediyl- $\alpha$ ,  $\omega$ -bis(dodecyldimethylammonium bromide) (C12CmC12Br2) with short spacer group can self-assemble into wormlike micelles.

Mixture of surfactant aqueous can exhibit much richer phase behavior than single surfactant and form relatively complicated aggregates. There are more and more reports on the studies of different combinations of mixed surfactant system viz. cationic/anionic [29-32], anionic/nonionic [33,34], anionic/zwitterionic [1,35-37], etc. Raghavan et al has reported the synergistic growth of wormlike micelles when there is an optimal surfactant tail lengths in anionic sodium oleate(NaOA) and cationic trimethylammonium bromide(C<sub>n</sub>TAB) systems[29]. Grillo et al find that in the mixture of anionic sodium bis(2-ethyl hexyl)sulfosuccinate AOT and nonionic Tetraethylene glycol monododecyl ether C12E4, Spherical micelles are present for AOT-rich composition while cylindrical micelles for C12E4-rich [33]. Similarly, various micelle aggregates can be achieved in the anionic/zwitterionic systems. Ghosh et al observed bilayer vesicles formed in dilute mixture solutions of zwitterionic surfactant C<sub>12</sub>GLY and anionic surfactant SDS in low molar fractions,  $X(=[C_{12}GLY]/[C_{12}GLY]+[SDS])$ , and fingerprint-like structure when X increased to  $X=0.5$  [35]. Qiao et al investigated that the wormlike micelle formed when the molar ratio X ( $[TPS]/[TPS]+[SDS]$ ) reach to  $X=0.6$  and  $Ca^{2+}$  concentration increased in the SDS/TPS/ $Ca(NO_3)_2$  system[1]. In this paper, atomistic MD simulations are performed to probe the effect of molar ratio and salt concentration to the anionic/zwitterionic mixed system.

## 2. Models and methods

### 2.1 Simulated parameters

All MD simulations were performed using the GROMACS 5.0.2 software package with the AMBER99 force field in this study. All those parameters which are not found in the AMBER99 force field such as the angle C-O-S or torsion C-C-C-O are selected from Hui Yan's[38] work. The simulations were run using the leap-frog algorithm with a 2-fs integration time step. Long-range electrostatic interactions were calculated using the particle mesh Ewald (PME) technique with a real-space cutoff distance of 1.2 nm. The Lennard-Jones interactions were truncated at a cutoff distance of 1.2 nm. All bond lengths were constrained using the linear constraint solver (LINCS) algorithm. The pressure was controlled using isotropic Parrinello-Rahman method at 1 bar with a coupling constant of 1.0 ps. Temperature control was achieved by using the Nose-Hoover algorithm with a coupling constant of 0.2 ps. All systems were simulated with three-dimensional periodic boundary conditions. First, each system was energy-minimized using 5000 steps of steepest descent method to relax any steric conflicts generated during system setup, then the system equilibrium was performed by a 1 ns MD run with positional restraints on all surfactants in the NVT ensemble at 340K, Finally, all the systems were performed a 60-ns simulation in the NPT ensemble at 300K. Visualizations of all molecular configurations are done in molecular graphics software, VMD.

### 2.2 Simulated System.

Our simulation systems include the ionic surfactants SDS, TPS, water molecules,  $Ca^{2+}$  and  $Cl^-$  ions. Water was described by the Tip3P model, which is known to provide a good representation of the dielectric properties as well as the thermodynamic properties. Atom charges in our work were use the Gaussian 09 package at the B3LYP/6-31+G\* level to optimize the structures of the two surfactants and calculate the ESP atomic charges. All the molecules were placed randomly within the simulation

box initially, as shown in Figure 1. In this study, we performed six simulated systems at fixed surfactant numbers but different ratios with 1Mol/L  $\text{Ca}^{2+}$  and six simulated systems at fixed ratio ( $X_{\text{TPS}}=0.6$ ) but different  $\text{Ca}^{2+}$  concentration respectively. All the systems are summarized in Table 1, Table 2.

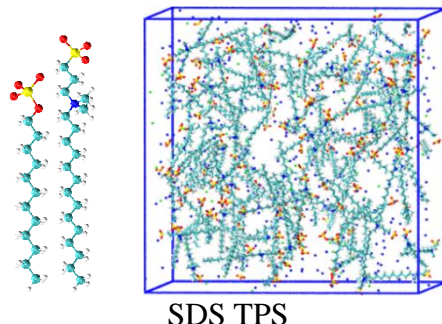


Figure 1: Left: SDS and TPS molecule, Right: An example of a random initial configuration of the 60SDS+90TPS in 1.0M  $\text{Ca}^{2+}$  system. Sulfur, oxygen, nitrogen, and carbon that belong to the surfactants are shown as yellow, red, blue, and cyan spheres, respectively

Table 1: Simulated systems I

System	TPS	SDS	Ca <sup>2+</sup>	CL <sup>-</sup>	Tip3p	X <sub>TPS</sub>	Box Size
A	0	150	300	600	13492	0	8×8×8nm <sup>3</sup>
B	30	120	300	600	13304	0.2	8×8×8nm <sup>3</sup>
C	60	90	300	600	13132	0.4	8×8×8nm <sup>3</sup>
D	90	60	300	600	12946	0.6	8×8×8nm <sup>3</sup>
E	120	30	300	600	12787	0.8	8×8×8nm <sup>3</sup>
F	150	0	300	600	12601	1	8×8×8nm <sup>3</sup>

Table 2: Simulated systems II

System	TPS	SDS	Ca <sup>2+</sup>	CL <sup>-</sup>	Tip3p	C	Box Size
a	90	60	0	0	13846	0	8×8×8nm <sup>3</sup>
b	90	60	30	60	13756	0.1	8×8×8nm <sup>3</sup>
c	90	60	150	300	13396	0.5	8×8×8nm <sup>3</sup>
d	90	60	300	600	12946	1.0	8×8×8nm <sup>3</sup>
e	90	60	450	900	12474	1.5	8×8×8nm <sup>3</sup>
f	90	60	600	1200	12059	2.0	8×8×8nm <sup>3</sup>

### 3. Results and discussion

#### 3.1 Molar ratio

##### 3.1.1 Aggregation Structure and Equilibration

We investigated the self-assembly processes of SDS and TPS mixtures at varying molar ratio ( $X_{\text{TPS}}=0, 0.2, 0.4, 0.6, 0.8, 1.0$ ) with the presence of 1mol/L  $\text{Ca}^{2+}$  by molecular dynamics simulations. By monitoring the trajectories, the micelles once formed are found to remain stable throughout the production run. The equilibration of the simulation systems is determined by monitoring the time-scaled potential energy of SDS/TPS mixtures. Figure 2 shows an example of

system D ( $X_{TPS}=0.6$ ) that the potential energy profile reaches a stable equilibrium after about 30 ns of simulation time. It indicates that 60ns is enough for our simulation. The snapshots of the system (A-F) configurations at the end of 60 ns equilibrium NPT are shown in Figure 3. From the figure, we can find that the surfactants assembled into micelles after a long MD run.

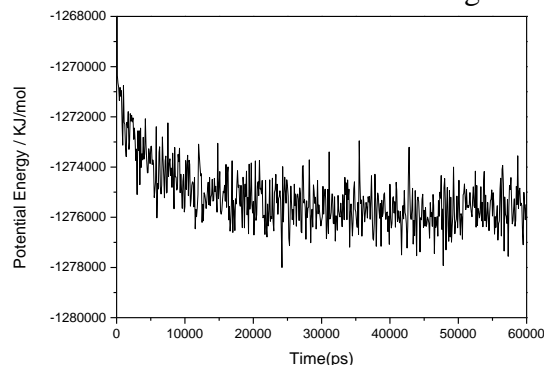


Figure 2: Time evolutions of the Potential energy with system D.

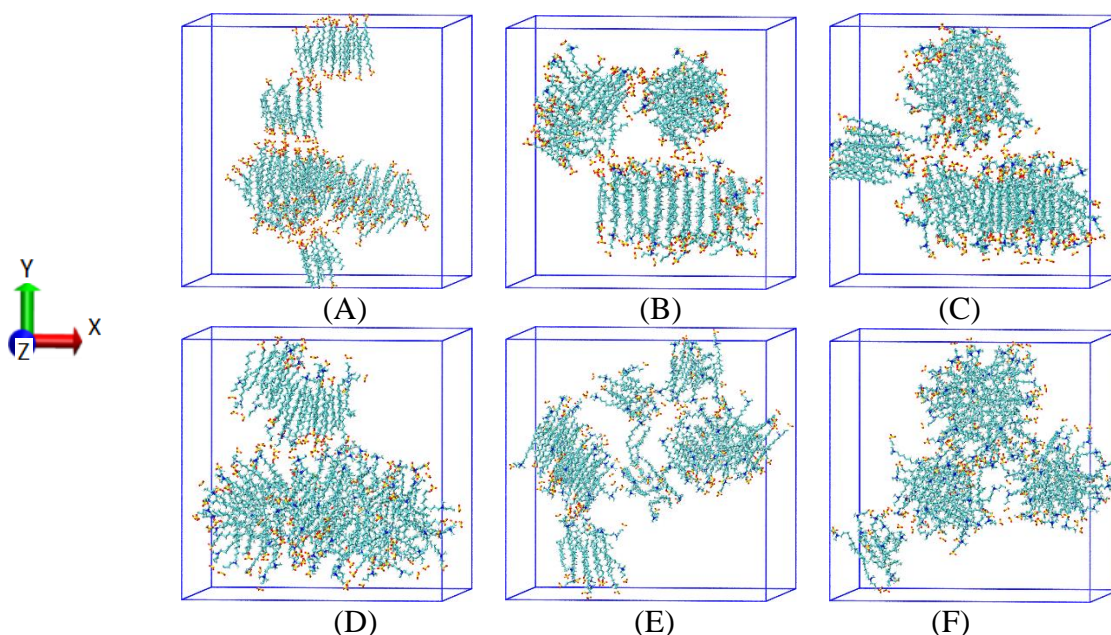


Figure 3: Snapshots of the configurations of SDS/TPS mixtures at varying  $X_{TPS}$  (system A-F) at  $t=60$ ns. Sulfur, oxygen, nitrogen, and carbon that belong to the surfactants are shown as yellow, red, blue, and cyan spheres, respectively; hydrogen atoms, water and other ions are omitted for clarity.

Table 3: Micelle structure statistics

Molar ratios( $X_{TPS}$ )	Number of micelle	Molecular number in micelles
0	4	98, 21, 20, 11
0.2	3	74, 40, 36
0.4	3	78, 53, 19
0.6	2	117, 33
0.8	6	42, 34, 26, 26, 13, 9
1.0	6	61, 29, 21, 16, 12, 11

From the Figure 3 we found the surfactant solutions formed various aggregation at different  $X_{TPS}$ . For SDS-rich systems, the predominant structure is interdigitated aggregation in which the SDS and TPS molecules are parallel settle aligned to each other (see Figure 3A-3C). As the  $X_{TPS}$  increased to

0.6, a wormlike micelle which SDS and TPS surfactants intersect arranged was formed, as shown in Figure 3D. However, with the increase of  $X_{TPS}$ , the wormlike micelle become unstable and split into several disperse spheres (see in Figure 3D-3F). We have statistic the micellar number and molecular number in Table 3, In SDS-rich systems ( $X_{TPS} < 0.6$ ), the number of micelle shown a decline tendency while the molecular number in the largest micelle increase with the increase of  $X_{TPS}$ . It indicates that with the increase of  $X_{TPS}$ , the systems formed less but larger micelles. And when  $X_{TPS} = 0.6$ , we found that the micellar number is the least but the size of the micelle is the largest. In TPS-rich systems ( $X_{TPS} > 0.6$ ), we can found more number but smaller size micelles. It reveals that the wormlike micelle is unstable and split into more small spheres when  $X_{TPS} > 0.6$ .

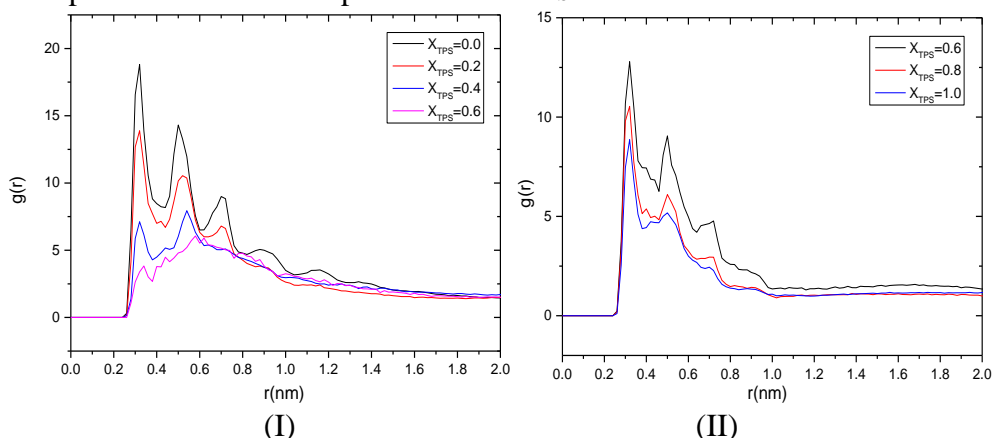


Figure 4: Radial distribution function between: SDS head group O to head group O in single and mixed solution (I) TPS head group O to head group O in single and mixed solution (II).

### 3.1.2 Molecular distribution

From a theoretical aspect, the molecular packing parameter[39]  $P = V_0 / a_0 * L$ , is generally used to rationalize or predict the aggregate shape Where  $V_0$  and  $L$  are the hydrophobic volume and length of the hydrophobic tail respectively,  $a_0$  is the average area of the head groups at the aggregation surface. The simple rule of  $0 \leq P \leq 1/3$  for spheres,  $1/3 \leq P \leq 1/2$  for wormlike and  $p \sim 1$  for bilayer, has been widely accepted to explaining amphiphilic self-assembly. Radial distribution function (RDF),  $g_{O-O}(r)$ , between head group oxygen atoms of the SDS and TPS molecules are shown in Figure. 4 for systems A–F. From Figure 4(I), A main peak appear at the same place located at  $r \approx 0.31$ nm in all systems ( $X_{TPS} \leq 0.6$ ), but the peak value becomes lower and lower with the increasing of TPS ratio. This implies that the molecular distribution between the SDS surfactants become more and more loose with the  $X_{TPS}$  increase. The loose micelle lead to a large  $a_0$  that decrease the value of  $P$ . That is why the structure of micelle transformed from interdigitate ( $P \sim 1$ ) to wormlike ( $1/3 \leq P \leq 1/2$ ). Similarly, the TPS-rich systems in Figure 4(II) also shows that the peak appear at the same place but peak value of the  $g_{O-O}(r)$  become lower and lower between TPS surfactants with the increasing of TPS ratio. It means that the micelle become more and more loose with the  $X_{TPS}$  increase. So the structure of micelle continue transformed from wormlike ( $1/3 \leq P \leq 1/2$ ) to spherical ( $P \leq 1/3$ ).

## 3.2 Salt concentration

### 3.2.1 Aggregation Structure

In the saline solutions, all the systems a-f were fixed at  $X_{TPS} = 0.6$  of 60 SDS and 90 TPS at varying salt concentration. As shown in Figure 5, the surfactants aggregate to several disperse interdigitate

micelles with SDS and TPS surfactants parallel arrange to each other in the salt-free system in Figure 5 (a). With the  $\text{Ca}^{2+}$  concentration increased to 0.1 and 0.5 mol/L (Figure 5 b and c), the micelle become more compact and bigger. This can be attributed to the fact that more  $\text{Ca}^{2+}$  added is sufficient to provide an effective screening of the SDS and TPS head group charges. When  $\text{Ca}^{2+}$  concentration increased to 1.0 mol/L, a thick and compact wormlike micelle is formed in Figure 5 (d). However, when  $\text{Ca}^{2+}$  concentration increased to 1.5 and 2.0 mol/L, the wormlike micelle split into some small clusters in Figure 5 e-f. It reveals that the excess  $\text{Ca}^{2+}$  ions will lead the micelle drastic fluctuate and break into some small clusters.

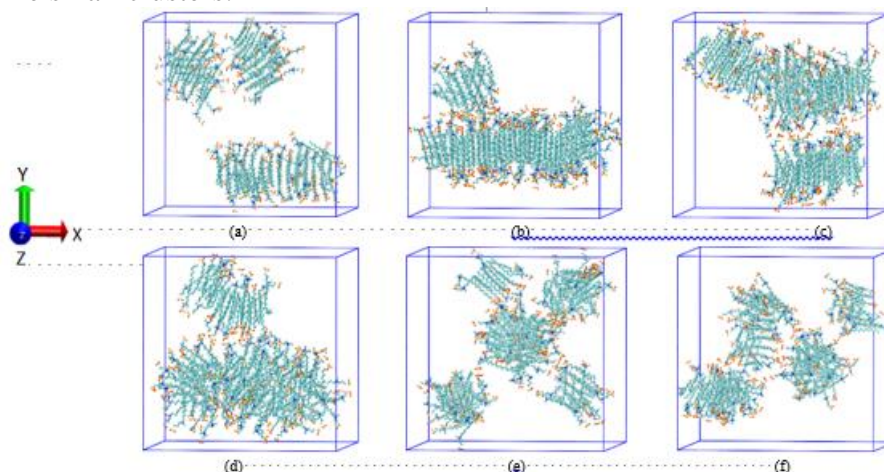


Figure 5: Snapshots of the configurations of 60 SDS and 90TPS mixtures in different  $\text{Ca}^{2+}$  solutions (system a-f) at  $t=60\text{ns}$ : (a) 0mol/L; (b) 0.1mol/L; (c) 0.5mol/L; (d) 1.0mol/L; (e) 1.5mol/L; (f) 2.0mol/L.

### 3.2.2 Molecular distribution and orientation

We calculate the density distribution of the SDS and TPS head group O along the Y axis in the largest micelle in system b and d. As show in Figure 6, In system b, we can see two distinct peaks for the density distribution of SDS and TPS head group O along the Y axis, it demonstrate that the molecular orientation of SDS and TPS are monotonous to parallel to the Y axis in the interdigitate micelle. The characteristic of the surfactant distribution cause the micelle more likely to relative slide to each other. While the distribution of the surfactants in the wormlike micelle are various orientation, and because of the ‘head’ in wormlike, the edge of the micelle is much stable to avoid the molecules to slide away. As show in Figure 7, we have statistic all the orientations of the molecules in the biggest micelle in system b and d. All the orientations are calculate the angle between the direction of surfactant and the Y axis as the green arrow shown in Figure 5. From the angle probability distribution, we found that most angles are  $\cong 10^\circ$  or  $\cong 170^\circ$  indicate that all the surfactants are basically parallel align to each other in system b, see Figure 7(left). While in the wormlike micelle, the probability distribution of the angle has a wide range from  $0^\circ$  to  $180^\circ$  indicates that the molecular orientation is various. So compare to interdigitate, wormlike micelle is not easy to slide away under the shear force and have a higher shear rate viscosity in the experiment [1].

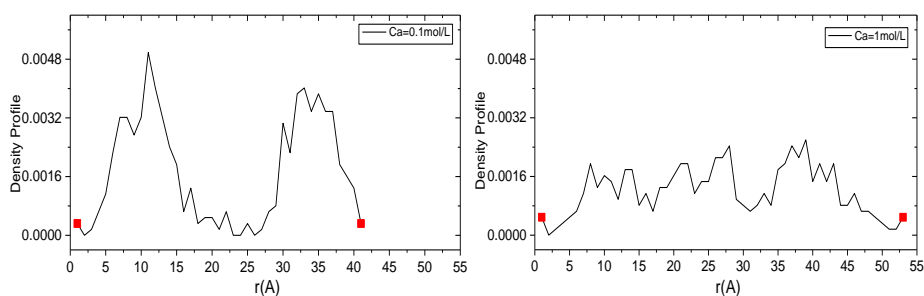


Figure 6: Density distributions of the SDS and TPS head group O in system b ( $\text{Ca}^{2+}=0.1\text{mol/L}$ ) and d ( $\text{Ca}^{2+}=1.0\text{mol/L}$ ) along the Y axis.

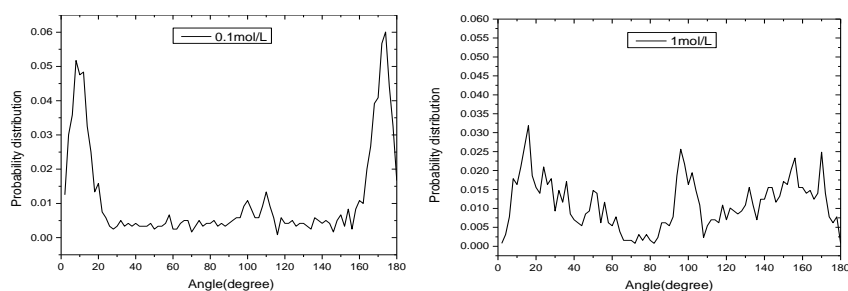


Figure 7: The orientations of the surfactants in the biggest micelle in system b ( $\text{Ca}^{2+}=0.1\text{mol/L}$ ) left; d ( $\text{Ca}^{2+}=1.0\text{mol/L}$ ) right

### 3.2.3 Salt bridge

Salt bridge could be a plausible explanation for the structural difference between the micelles formed in different  $\text{Ca}^{2+}$  concentration. To study this aspect, the probability of a salt bridge between nearest neighbor head group pairs has been assessed. We defined a salt bridge to exist when two head group S atom were bridged by one  $\text{Ca}^{2+}$  ion while the  $\text{Ca}^{2+}$  resides within a distance  $R_{\text{cut}}=0.45\text{nm}$  from two S atoms in the surfactants. The specific value for  $R_{\text{cut}}=0.45\text{nm}$  is based on the radial distribution functions corresponding to  $\text{Ca}^{2+}$  condensation radii measured from the S-atom in the head group in Figure 8. Figure 9(I) illustrates one  $\text{Ca}^{2+}$  bridging between two surfactant head group which is selected randomly in system d. Then we calculate the number of salt bridge in different salt concentration, as show in Figure 9(II). The number of salt bridge is rapidly increased from salt-free system to  $0.5\text{mol/L}$   $\text{Ca}^{2+}$  systems. That means more and more  $\text{Ca}^{2+}$  ions bound to the surfactant head groups to screen electrostatic interaction. However, the salt bridge number in  $0.5\text{mol/L}$  system increased slowly to  $1.0\text{mol/L}$  systems indicates that the number of  $\text{Ca}^{2+}$  ions is already enough to screen electrostatic interaction. So when  $\text{Ca}^{2+}$  concentration increased from  $1\text{mol/L}$  to  $1.5$  and  $2.0\text{mol/L}$ , too many  $\text{Ca}^{2+}$  ions bound to the head of surfactant lead to a high local charge density. That induce the wormlike micelle unstable and split into sphere micelles.

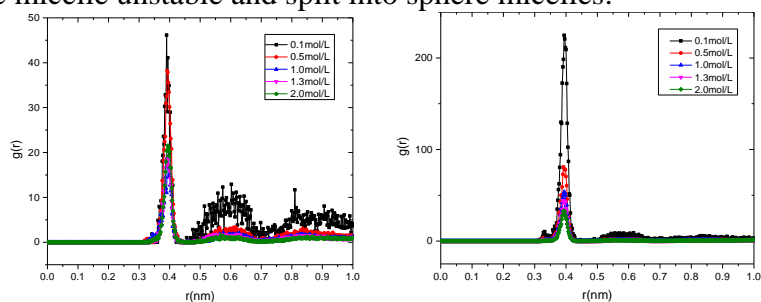


Figure 8: Radial distribution function between: (left) S atom in SDS and Ca ions; (right) S atom in TPS and Ca ions at varying  $\text{Ca}^{2+}$  concentration

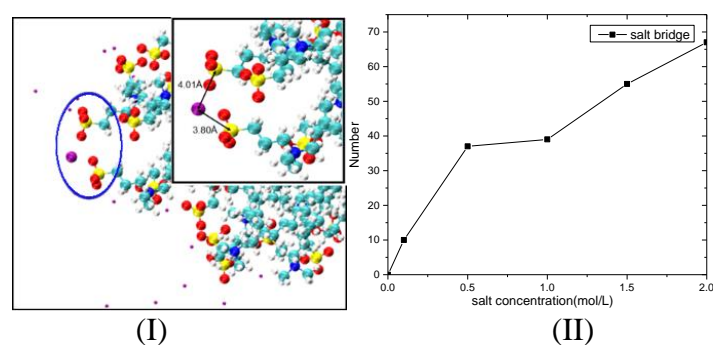


Figure 9: (I): Salt bridging observed corresponds to the binding of two head group with  $\text{Ca}^{2+}$ , the color code is the same as Figure 3 (purple sphere is  $\text{Ca}^{2+}$ ). The upper-right inset shows highlighted by the blue circled area on an enlarged scale; (II): The number of salt bridge in different salt concentration

#### 4. Conclusion

We have explored the formation of micellar aggregates in systems of different molar ratio with 1 mol/L  $\text{Ca}^{2+}$  solution, and a constant molar ratio  $X_{\text{TPS}}=0.6$  at varying  $\text{Ca}^{2+}$  concentration for SDS/TPS mixtures. The results show that the potential shape evolution rule in the SDS–TPS– $\text{Ca}^{2+}$  system with different molar ratio  $X_{\text{TPS}}$  was interdigitate-wormlike-sphere. Only when  $X_{\text{TPS}}$  increased to 0.6, a compact and cylindrical wormlike micelle is formed in our simulation. As the effect of salt concentration, we investigated that surfactant solutions can form interdigitate micelle in low salt concentration. With the  $\text{Ca}^{2+}$  increased, more and more  $\text{Ca}^{2+}$  ions distribute around the negative head group to neutralize the electrostatic repulsion lead to a transition of interdigitate to wormlike. But too many  $\text{Ca}^{2+}$  added will make the local charge density too high to make the wormlike unstable and split into small clusters. So we conclude that there exist an appropriate molar ratio and salt concentration to form wormlike micelle in the mixed surfactant solutions.

#### Acknowledgements

The work was supported by National Natural Science Foundation of China (Grant No. 11274122).

#### References

- [1] Qiao, Y., et al. (2011) Metal-Driven Viscoelastic Wormlike Micelle in Anionic/Zwitterionic Surfactant Systems and Template-Directed Synthesis of Dendritic Silver Nanostructures. *Langmuir*. 27, 1718-1723.
- [2] Israelachvili, J. N., D. J. Mitchell, and B. W. Ninham. (1976) Theory of self-assembly of hydrocarbon amphiphiles into micelles and bilayers. *Journal of the Chemical Society, Faraday Transactions 2: Molecular and Chemical Physics*. 72, 1525-1568.
- [3] Cates, M. E. and S. J. Candau. (1990) Statics and dynamics of worm-like surfactant micelles. *Journal of Physics: Condensed Matter*. 2, 6869-6892.
- [4] Abdel-Rahem, R. (2008) The influence of hydrophobic counterions on micellar growth of ionic surfactants. *Advances in Colloid and Interface Science*. 141, 24-36.
- [5] Marrink, S. J., D. P. Tieleman, and A. E. Mark. (2000) Molecular dynamics simulation of the kinetics of spontaneous micelle formation. *Journal of Physical Chemistry B*. 104, 12165-12173.
- [6] Morrissey, D. V., et al. (2005) Potent and persistent in vivo anti-HBV activity of chemically modified siRNAs. *Nature Biotechnology*. 23, 1002-1007.
- [7] Wei, W. and E. S. Yeung. (2001) DNA capillary electrophoresis in entangled dynamic polymers of surfactant molecules. *Analytical Chemistry*. 73, 1776-1783.
- [8] Bagaria, H. G., G. C. Kini, and M. S. Wong. (2010) Electrolyte Solutions Improve Nanoparticle Transfer from Oil to Water. *Journal of Physical Chemistry C*. 114, 19901-19907.

- [9] Moren, A. K., et al. (1999) Microstructure of protein-surfactant complexes in gel and solution - An NMR relaxation study. *Langmuir*. 15, 5480-5488.
- [10] Shukla, A. and H. Rehage. (2008) Zeta potentials and debye screening lengths of aqueous, viscoelastic surfactant solutions (cetyltrimethylammonium bromide/sodium salicylate system). *Langmuir*. 24, 8507-8513.
- [11] Golemanov, K., et al. (2008) Surfactant mixtures for control of bubble surface mobility in foam studies. *Langmuir*. 24, 9956-9961.
- [12] Majhi, P. R., et al. (2004) Coexistence of spheres and rods in micellar solution of dodecyltrimethylamine oxide. *Journal of Physical Chemistry B*. 108, 5980-5988.
- [13] Magid, L. J., et al. (1997) Effect of counterion competition on micellar growth horizons for cetyltrimethylammonium micellar surfaces: Electrostatics and specific binding. *Journal of Physical Chemistry B*. 101, 7919-7927.
- [14] Hedin, N., I. Furo, and P. O. Eriksson. (2000) Fast diffusion of the Cl<sup>-</sup> ion in the headgroup region of an oppositely charged micelle. A Cl-35 NMR spin relaxation study. *Journal of Physical Chemistry B*. 104, 8544-8547.
- [15] Zehl, T., et al. (2006) Monte Carlo simulations of self-assembled surfactant aggregates. *Langmuir*. 22, 2523-2527.
- [16] Howes, A. J. and C. J. Radke. (2007) Monte Carlo simulations of Lennard-Jones nonionic surfactant adsorption at the liquid/vapor interface. *Langmuir*. 23, 1835-1844.
- [17] Khurana, E., S. O. Nielsen, and M. L. Klein. (2006) Gemini surfactants at the air/water interface: A fully atomistic molecular dynamics study. *Journal of Physical Chemistry B*. 110, 22136-22142.
- [18] Bandyopadhyay, S. and J. Chanda. (2003) Monolayer of monododecyl diethylene glycol surfactants adsorbed at the air/water interface: A molecular dynamics study. *Langmuir*. 19, 10443-10448.
- [19] Jang, S. S. and W. A. Goddard. (2006) Structures and properties of newton black films characterized using molecular dynamics simulations. *Journal of Physical Chemistry B*. 110, 7992-8001.
- [20] Tummala, N. R. and A. Striolo. (2008) Role of counterion condensation in the self-assembly of SDS surfactants at the water-graphite interface. *Journal of Physical Chemistry B*. 112, 1987-2000.
- [21] Mohanty, S., H. T. Davis, and A. V. McCormick. (2001) Complementary use of simulations and free energy models for CTAB/NaSal systems. *Langmuir*. 17, 7160-7171.
- [22] Wang, Z. and R. G. Larson. (2009) Molecular Dynamics Simulations of Threadlike Cetyltrimethylammonium Chloride Micelles: Effects of Sodium Chloride and Sodium Salicylate Salts. *Journal of Physical Chemistry B*. 113, 13697-13710.
- [23] Sangwai, A. V. and R. Sureshkumar. (2011) Coarse-Grained Molecular Dynamics Simulations of the Sphere to Rod Transition in Surfactant Micelles. *Langmuir*. 27, 6628-6638.
- [24] Sangwai, A. V. and R. Sureshkumar. (2012) Binary Interactions and Salt-Induced Coalescence of Spherical Micelles of Cationic Surfactants from Molecular Dynamics Simulations. *Langmuir*. 28, 1127-1135.
- [25] Sammalkorpi, M., M. Karttunen, and M. Haataja. (2007) Structural properties of ionic detergent aggregates: a large-scale molecular dynamics study of sodium dodecyl sulfate. *Journal of Physical Chemistry B*. 111, 11722-11733.
- [26] Sammalkorpi, M., M. Karttunen, and M. Haataja. (2009) Ionic Surfactant Aggregates in Saline Solutions: Sodium Dodecyl Sulfate (SDS) in the Presence of Excess Sodium Chloride (NaCl) or Calcium Chloride (CaCl<sub>2</sub>). *Journal of Physical Chemistry B*. 113, 5863-5870.
- [27] Velinova, M., et al. (2011) Sphere-to-Rod Transitions of Nonionic Surfactant Micelles in Aqueous Solution Modeled by Molecular Dynamics Simulations. *Langmuir*. 27, 14071-14077.
- [28] Zana, R. and Y. Talmon. (1993) Dependence of aggregate morphology on structure of dimeric surfactants. *Nature*. 362, 228-230.
- [29] Raghavan, S. R., G. Fritz, and E. W. Kaler. (2002) Wormlike micelles formed by synergistic self-assembly in mixtures of anionic and cationic surfactants. *Langmuir*. 18, 3797-3803.
- [30] Koshy, P., et al. (2011) Unusual Scaling in the Rheology of Branched Wormlike Micelles Formed by Cetyltrimethylammonium Bromide and Sodium Oleate. *Journal of Physical Chemistry B*. 115, 10817-10825.
- [31] Lin, Y., et al. (2008) pH-Regulated Molecular Self-Assemblies in a Cationic-Anionic Surfactant System: From a "1-2" Surfactant Pair to a "1-1" Surfactant Pair. *Langmuir*. 24, 13918-13924.
- [32] Yakovlev, D. S. and E. S. Boek. (2007) Molecular dynamics simulations of mixed cationic/anionic wormlike micelles. *Langmuir*. 23, 6588-6597.
- [33] Grillo, I. and J. Penfold. (2011) Self-Assembly of Mixed Anionic and Nonionic Surfactants in Aqueous Solution. *Langmuir*. 27, 7453-7463.
- [34] Garamus, V. M. (2003) Formation of mixed micelles in salt-free aqueous solutions of sodium dodecyl sulfate and C12E6. *Langmuir*. 19, 7214-7218.
- [35] Ghosh, S., D. Khatua, and J. Dey. (2011) Interaction Between Zwitterionic and Anionic Surfactants: Spontaneous Formation of Zwitterionic Vesicles. *Langmuir*. 27, 5184-5192.
- [36] Sarmiento-Gomez, E., D. Lopez-Diaz, and R. Castillo. (2010) Microrheology and Characteristic Lengths in Wormlike Micelles made of a Zwitterionic Surfactant and SDS in Brine. *Journal of Physical Chemistry B*. 114, 12193-12202.

- [37] Chen, J. F. and J. C. Hao. (2013) *Molecular dynamics simulation of cetyltrimethylammonium bromide and sodium octyl sulfate mixtures: aggregate shape and local surfactant distribution. Physical Chemistry Chemical Physics. 15, 5563-5571.*
- [38] Yan, H., et al. (2010) *Effect of  $\text{Ca}^{2+}$  and  $\text{Mg}^{2+}$  Ions on Surfactant Solutions Investigated by Molecular Dynamics Simulation. Langmuir. 26, 10448-10459.*
- [39] Israelachvili, J. N.(1977), D. J. Mitchell, and B. W. Ninham, *Theory of self-assembly of lipid bilayers and vesicles. Biochimica et biophysica acta. 470, 185-201.*